IEEE Access
Multidisciplinary ⋮ Rapid Review ⋮ Open Access Journal

Received 8 August 2023, accepted 26 August 2023, date of publication 30 August 2023, date of current version 7 September 2023.

Digital Object Identifier 10.1109/ACCESS.2023.3310407

RESEARCH ARTICLE

A Wideband Gap Waveguide-Fed 16-Element Circularly Polarized Patch Antenna Array

ABDULLAH J. ALAZEMI [1], (Member, IEEE), **ALI FARAHBAKHSH** [2], AND **DAVOUD ZARIFI** [3]
[1]Department of Electrical Engineering, Faculty of Engineering and Petroleum, Kuwait University, Safat 13060, Kuwait
[2]Department of Electrical and Computer Engineering, Graduate University of Advanced Technology, Kerman 7631818356, Iran
[3]School of Electrical and Computer Engineering, University of Kashan, Kashan 8731753153, Iran

Corresponding author: Abdullah J. Alazemi (aalazem.ku@ku.edu.kw)

This work was supported by Kuwait University under Grant EE03/21.

ABSTRACT This paper presents a design of a 4 × 4 circularly polarized (CP) patch antenna array based on gap waveguide (GW) sequential feeding network. The proposed antenna single element consists of an aperture coupled circular patch antenna. A two-level sequential feeding network, that is used to enhance the polarization bandwidth, is designed, and investigated. The GW technology is employed to decrease the feeding network loss; and consequently, to achieve a low-loss antenna array. The antenna input port is a standard waveguide (WR-28), and it is coupled to the GW-based feed network using an appropriate transition. The proposed array is printed on RT5880 substrate, (with a relative permittivity of 2.2). The measured and simulated results show that both input $|S_{11}|$ and axial ratio bandwidths are greater than 30% over the frequency range of 25.8-35 GHz. The maximum gain is 18 dBic. The proposed work is considered a great choice for millimeter-wave applications.

INDEX TERMS Circular polarization, patch antenna, millimeter wave, gap waveguide.

I. INTRODUCTION

Recently, millimeter waves (mmWaves) have attracted more attention from the various researchers because of its practical advantages and utilities for various future applications such as high data-rate communications, high definition (HD) video transmission, HD multimedia interfaces, automotive applications and vehicle radars [1]. As a key component of mmWaves communication system, design and development of appropriate antennas with desired specifications is required. The employed antenna should offer excessive gain, polarization, and radiation performance in the broad frequency ranges. Another crucial element affecting the system cost is the robustness of the antenna and the convenience of integration with different microwave components.

Circularly polarized (CP) antenna arrays are required for mmWaves satellite communications, point-to-point cellular communications, and other municipal applications to remove multipath interferences and unmatched polarization. Thus, millimeter wave CP antenna arrays have been very attractive topic for researchers. There are two general methods to design a CP antenna array. In the first method, elements with CP radiation are used and they are fed in the array in phase and with same amplitude. In this method, the array axial ratio (AR) bandwidth, in the best case, will be equal to the AR bandwidth of the element, which is generally not acceptable for some applications. Various elements have been used to create a CP antenna array, including U-shaped slot patch [2], a complementary Yagi antenna [3], a slot-fed rotated dipole antenna [4], magneto-electric dipole [5], wheel-shaped element [6], dielectric resonator antenna [7] and cross-slot excited patch [8]. In the second method, a sequential feeding is used. In this method, CP radiation can be created by using the rotation of the elements and by providing a sequential rotation phase for each element, which makes the polarization bandwidth of the array much wider than the bandwidth of its element. In this case, even elements with linear polarization can be used [9]. Various structures for realizing sequential feeding have been presented in the literature, for example, microstrip-fed array antennas [8], [9], [10], [11], substrate

The associate editor coordinating the review of this manuscript and approving it for publication was Giorgio Montisci.

This work is licensed under a Creative Commons Attribution-NonCommercial-NoDerivatives 4.0 License.
For more information, see https://creativecommons.org/licenses/by-nc-nd/4.0/

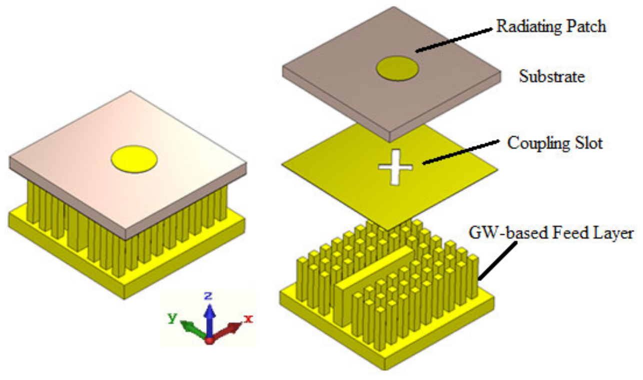

FIGURE 1. (a) A perspective view of the structure of proposed CP antenna subarray. (b) an exploded view.

integrated waveguides (SIW) feeding arrays [12], [13], [14], [15], [16], [17], [18], [19], conventional waveguide feeding arrays [20], [21], [22].

Most antenna arrays with CP radiation suffer from low AR bandwidth since low bandwidth causes significant and effective limitations in the communication links. Sequential feeding network is usually applied to increase the array AR bandwidth and obtain wideband CP radiation. Due to its complexity, normally the sequential feeding method is implemented only on one level, and for realizing larger arrays, in-phase feeding is used. In addition, the PCB-based CP antenna arrays are compact, lightweight, easy to fabricate, capable to integrate with various passive and active microwave structures. The main limitation factors affecting their performance are the low-power handling, the high dielectric loss, and the leakage wave propagation at high frequencies. Slotted waveguide arrays are the maximum appealing applicants for broadband and high gain performance in millimeter-wave applications. They do not suffer from dielectric loss and are suitable for high gain and high-performance applications. However, the feeding network has become too complex and cumbersome and requires precise and high-cost fabricating. In particular, it ias a challenge to achieve a good electrical contact between the different antenna layers.

Gap waveguide (GW) technology was introduced in 2010 to provide a good electrical contact when performing mechanical assembly [23]. The recent research articles show a demonstration of some GW-based antennas with passive components [24], [25], [26], [27], [28]. Several GW-based antenna arrays with CP radiation have been proposed [29], [30], [31], [32], [33], [34], [35]. In [30], a SIGW-fed 4-element circularly polarized antenna array is presented with an impedance bandwidth (IBW) of 25.6%, AR bandwidth (ARBW) of 19%, and peak gain of 11.53 dBic for Ku-band applications. In [31], an 8×8 antenna array with CP radiation and the maximum efficiency of 85% has been proposed. In that 3-layer design, a ridge gap waveguide-based sequential rotation technique has been used to excite the cavity layer, which has been employed for feeding the radiation slots. Due to the use of the cavity layer, the bandwidth of the structure has been limited to about 22%. In [32], the design of a 64-array antenna had been documented that has a 29 dBic peak gain, minimum aperture efficiency of 34% for 19 to 30 GHz. In that design, the embedded CP bold-C spiral elements have been fed by a complicated 7-layer dielectric-based inverted microstrip GW-based feed network. A 3-layer CP 16-element antenna array working from 27.5 GHz to 31 GHz (13% bandwidth) with a maximum gain of 19.24 has been presented in [33]. In general, it can be said that the aforementioned structures are relatively complicated because they use multilayer structures that have a complex and high-cost fabricating process. In addition, some of them exhibit a narrow relative bandwidth. These properties are strong drawbacks that prevent their usage in broadband millimeter-wave systems.

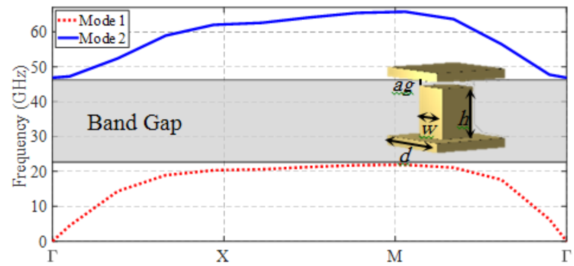

FIGURE 2. Dispersion unit cell diagram of the periodic structure.

In this work, a study is done to use GW technology to design a GW-based CP antenna based on simple planar and high bandwidth structures. This contribution shows a design of a millimeter-wave array with CP radiation using GW technology. The proposed antenna is a microstrip patch array with a sequential feeding network and ridge GW structure. As the feeding network is considered one of the main loss parts in any array system, ridge gap waveguide is utilized to eliminate the feeding losses and therefore, achieve a high-performance antenna array. Compared to the 3-layer structure presented in [31], the proposed antenna in this paper has a two-layer structure, which a PCB-based layer is used as the radiation layer for two reasons: First, by removing the cavity layer, compacting the feeding network and using aperture-coupled patches, the bandwidth of the antenna has increased and reaches about 30%; And secondly, removing the metallic cavity and radiation layers leads to a simple and low-price fabrication procedure.

The article is organized based on the following sections: In Section II, the CP antenna element is presented. In Section III, the design of sequential power divider is demonstrated. In Section IV, the final design of 16-element antenna array is manufactured, and the measurement results are shown.

II. WIDEBAND CP ANTENNE ELEMENT

The element used in the presented design has right-handed CP radiation, whose structure is illustrated in Fig. 1. The radiating element is a circular patch printed on a substrate

TABLE 1. Design parameters of the proposed CP antenna element.

Parameter	Value (mm)
Radius of the circular patch	1.3
Length of long slot	3.8
Length of short slot	2.1
Width of Slots	0.5
Distance from the ridge end to slots centers	1.45

that is fed through a cross-shaped slot that is in the form of two orthogonal slots that are rotated 45°. The need of the 45° cross-shaped rotation is to excite both slots by the ridge waveguide. Otherwise, if there is no rotation, only one of the slots will be excited. The different length of two slots causes a phase difference of 90° between the two slots and results in a circularly polarized radiation. The illustrated structure in Fig. 1 is utilized to produce right-handed circular polarization (RHCP). On the other hand, left-handed circular polarization (LHCP) can be obtained by changing the positions of short and long slots. The feeding layer consists of a metallic ridge that is surrounded by a texture of pins to confine the waves only on the ridge.

The dimensions of the pins must be precisely chosen to create a stop-band that covers the desired frequency band. The dimensions of the pins are chosen as follows: $w = 0.45$ mm, $h = 2$ mm, $d = 1$ mm, $ag = 20$ μm. The width of the ridge is 0.8 mm, and its height is slightly less than the height of the pins and equal to 1.9 mm. The stop-band of the pin structure is simulated using period boundary condition in CST Microwave Studio as shown in Fig. 2, the result indicates that there is no wave propagation from 22 to 47 GHz frequency range, and therefore, a stop-band had been created.

The antenna is printed on RT5880 material that has a relative permittivity equal to 2.2, a loss tangent of 0.0009, and a thickness of 0.78 mm. It is worth mentioning that the major losses of the PCB-based antennas are in the feeding part, where the wave must travel in a long way on the substrate. In the proposed structure, the antenna loss is negligible as the feeding network is designed using gap waveguide.

To obtain low reflection at antenna input port and wide axial ratio bandwidth (AR<3 dB), the sub-array parameters should be optimized. These parameters include the width of the slots, the length of the short and long slots, the circular patch radius, and the distance from the ridge end to the cross-shaped slot center. The proposed antenna element is simulated and optimized by Trust Region Framework method in CST Microwave Studio, and the optimum parameters are mentioned in Table 1. The simulated results of $|S_{11}|$, AR and gain for the proposed antenna element are plotted in Fig. 3. The antenna matching is acceptable from 25.5-33.5 GHz with the peak gain of 7.2 dBic. Also, the AR is smaller than 3 dB in the frequency range 29.5-31 GHz. The electric field distribution of subarray at 30 GHz is depicted in Fig. 4. At $t = 0$, T/4, 2T/4, and 3T/4, the rotation of electric fields can be seen which proves the CP radiation.

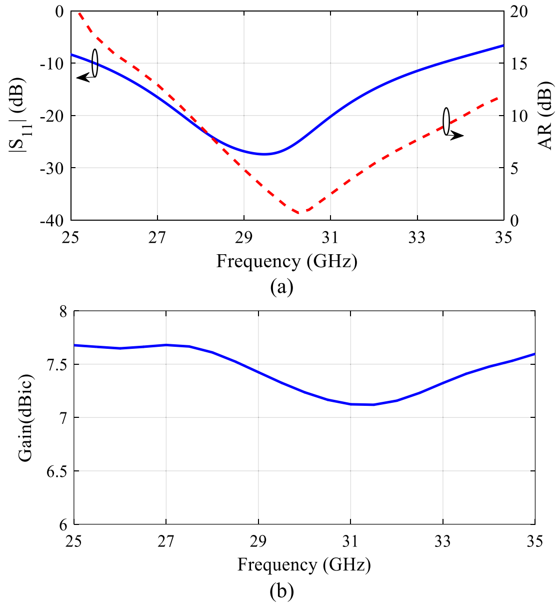

FIGURE 3. (a) Simulated $|S_{11}|$, AR and (b) gain of CP antenna element.

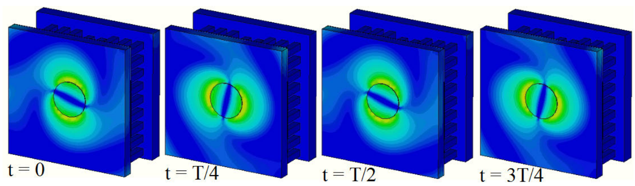

FIGURE 4. The distribution of electric field on the antenna subarray at 30 GHz.

III. DESIGN OF SEQUENTIAL POWER DIVIDER

In the proposed design, the sequential feeding method is used to increase the AR bandwidth. In this method, the array elements are rotated by 90° relative to each other, and their excitation are applied 90° phase difference relative to each other. The antenna array will radiate LHCP or RHCP, by applying a phase difference in a clockwise or counter-clockwise, respectively. In the sequential feeding technique, the polarization of the element can also be linear. But if a CP element is used, it will result in increasing the polarization bandwidth.

In this work, the design of an antenna array with 16 radiating elements is proposed in which a two-level sequential feeding is used to enhance the AR bandwidth as much as possible. Fig. 5(a) shows the first level sequential feeding power divider. In the simulation, some ports are placed at the power divider outputs. But, in the final design, the outputs will be connected to the proposed antenna element in the previous section. As depicted in Fig. 5(a), the wave from the input port is divided into two parts with similar amplitudes. The length difference of the first T-junction arms (L_1 and L_2) causes a phase difference of 180°. Also, the length difference of the L_3 and L_4 arms causes a 90° phase difference, which ultimately creates a clockwise phase sequence. To achieve good impedance matching in the ridge T-junctions,

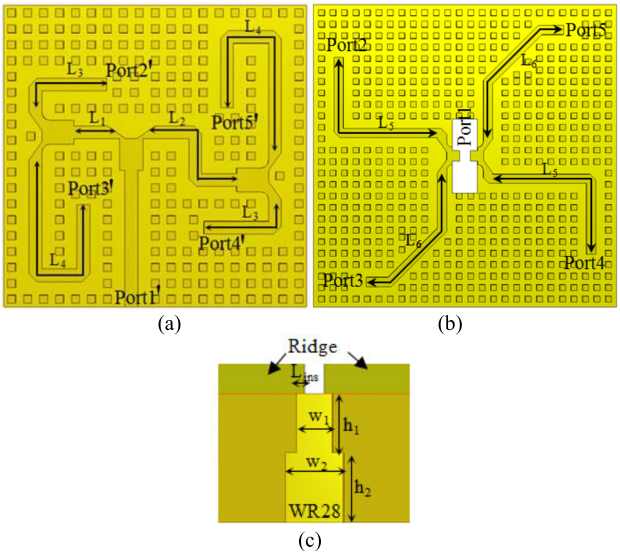

FIGURE 5. The configuration of (a) the first level, (b) the second level sequential feeding networks and (c) cross section of WR28 to ridge transition.

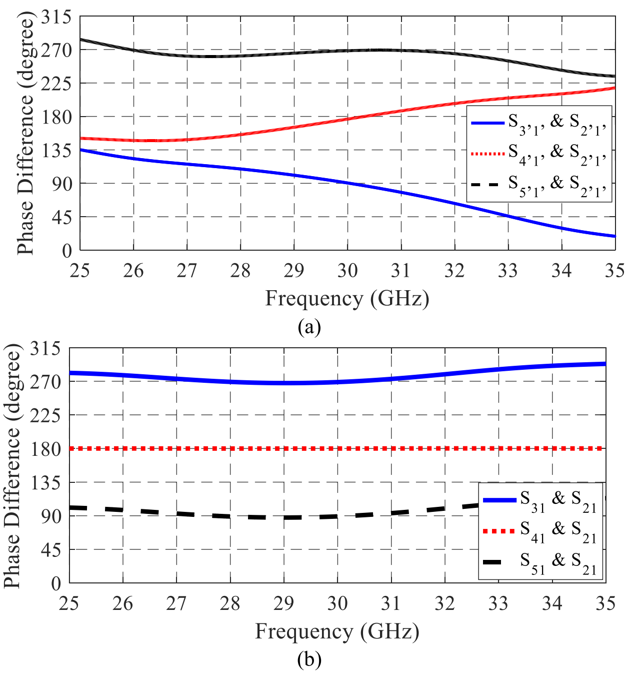

FIGURE 6. Phase differences of S-parameters of sequential feeding networks versus frequency. (a) First level. (b) Second level.

quarter-wave transformers are used, and the details of their design have been discussed in [20]. The phases differences of output ports are presented in Fig. 6(a). It is noticed that the 90° phase difference of the outputs at the center frequency of 30 GHz is exactly achieved. The phase differences are changed by changing the frequency as the phase differences are achieved using extra length in the arms.

The second level of the feeding network is demonstrated in Fig. 5(b) that consists of two ridge T-junctions and

TABLE 2. Design parameters of the proposed CP antenna element.

Parameter	Value (mm)	Parameter	Value (mm)
L_1	2.99	L_2	7.99
L_3	4.48	L_4	11.98
L_5	15.55	L_6	13.05
h_1	3.65	h_2	4.34
w_1	2.2	w_2	3.556
L_{ins}	0.85	Patches Spacing	8.5

a waveguide-to-ridge transition in the center. The length differences of L_5 and L_6 causes a 90° phase difference. The waveguide-to-ridge transition converts the rectangular waveguide propagation mode into the ridge one and is an out-of-phase power divider. The details of the transition are given in [20]. Since the outputs of the transition have 180° phase difference, there is no need for an extra 180° phase shifter and therefore, the feeding network becomes much simpler. The phase differences of the second level feeding network outputs are shown in Fig. 6(b). According to the results, the consecutive phase difference of 90° at 30 GHz is obtained. By comparing Figs. 6(a) and 6(b), it can be seen that the phase deviations versus the frequency in the second level is much lower than the first one as the 180° phase difference of the transition outputs is not dependent on the frequency.

The proposed design should be excited using a standard WR-28 waveguide flange. Due to structure compactness, the waveguide-to-ridge transition width is smaller than the standard WR-28 waveguide. Therefore, a matching section including two steps is designed as shown in Fig. 5(c) and by tuning the width and height of the steps, the matching is achieved. The design parameters of the whole antenna are given in Table 2.

The electric field distribution of the feeding network at frequency of 30 GHz is illustrated in Fig. 7. Simulated results can be used to demonstrate that the 90° phase differences between the different outputs in the feeding structure can provide the desired performance to achieve an antenna with CP radiation.

IV. FULL ARRAY DESIGN, FABRICATION, AND MEASUREMENT

A. CONFIGURATION OF 4 × 4-ELEMENT ARRAY

The final design structure of the proposed antenna array is obtained by combining the antenna element and the first and second level feeding networks. The proposed array layout is presented in Fig. 8 and includes the feeding network and the radiating layer. CST Studio Suite is used to simulate the final design structure.

It is worth mentioning that antenna design procedure is done in such a way to reduce the fabrication cost. Therefore, the feeding network is compacted to a RGW single layer, and the sensitivity of the antenna performance on the fabrication tolerances are considered during the design procedure. To show this issue, the effects of the mechanical tolerances in

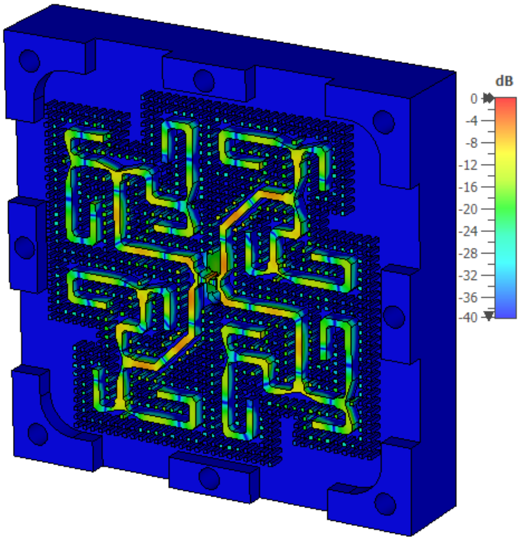

FIGURE 7. The distribution of electric field on the feed network at 30 GHz.

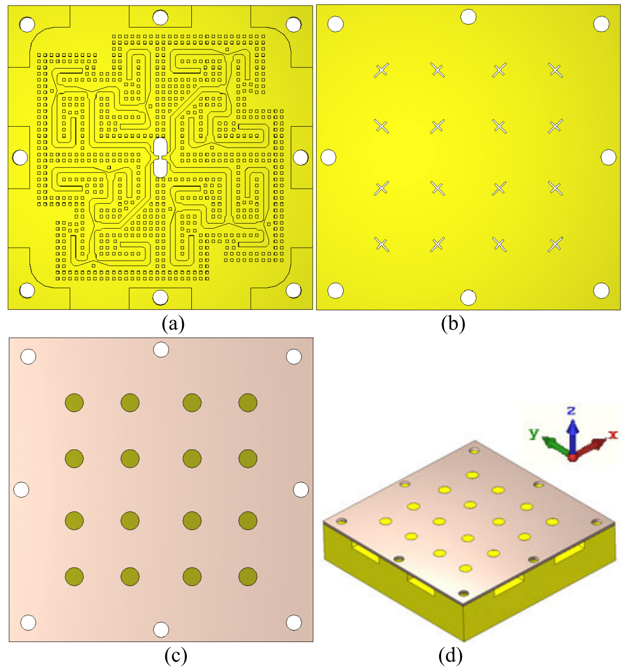

FIGURE 8. A layout of the proposed CP 4 × 4-element array. (a) Feeding Layer. (b) The bottom and (c) top view of the radiating Layer. (d) Perspective view.

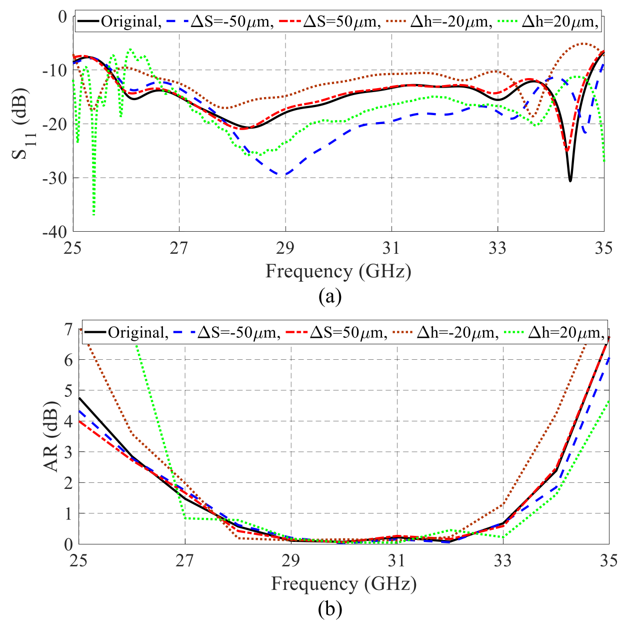

FIGURE 9. Effects of the fabrication tolerances on the antenna (a) matching and (b) axial ratio.

horizontal and vertical directions (ΔS and Δh) on the antenna matching and AR are simulated which are depicted in Fig. 8. According to the simulation results, although the antenna matching and AR change slightly with the tolerances, they are still acceptable with $\Delta S = \pm 50\mu m$ and $\Delta h = \pm 20\mu m$. Therefore, the antenna can be fabricated using a low-cost technique.

B. PROTOTYPE FABRICATION AND MEASUREMENT

A prototype of the proposed antenna system is manufactured to validate the simulated results. The structure's overall size is $50 \times 50 \times 11$ mm^3 (that includes the alignment pins and a few screws spaces) while the aperture size is 34×34 mm^2. Pictures of the disassembled parts and the assembled structure are presented in Fig. 9. The antenna input reflection coefficient is measured by a Keysight network analyzer N5225B.

The simulated and measured results for $|S_{11}|$ and AR are illustrated in Fig. 10 (a). It can be observed that the antenna input port reflection coefficient is smaller than -10 dB at 25.6-35 GHz which indicates an input bandwidth of 31%. The measured antenna axial ratio is lower than 3 dB from 25.8-35 GHz frequency range, which is equivalent to an ARBW of 30.3%. Fig. 10(b) demonstrated the boresight gain and radiation efficiency of the proposed antenna array at different frequencies. It is found that highest gain of the antenna occurred at the frequency of 30 GHz, and it is equal to 18 dBic. The antenna array efficiency is computed by using the simulated directivity and the measured gain. The maximum antenna efficiency at 29 GHz is about 90% while the maximum aperture efficiency is about 93%. It is also found that by changing the frequency from the central frequency, the antenna radiation efficiency (and gain) decreases, this is due to the change in the sequential feeding network phase.

The slight differences between the simulated and measured results could be due to variations in metal conductivity, the manufacturing tolerance, some misalignments between the different layers, and some measurement errors. A significant improvement of the CP radiation is noticed when comparing the AR of the antenna element and the 16-element array. This can be attributed to the excellent performance of the sequential feeding network.

The simulated and measured radiation patterns are presented in Fig. 12. The measured first sidelobe levels in both

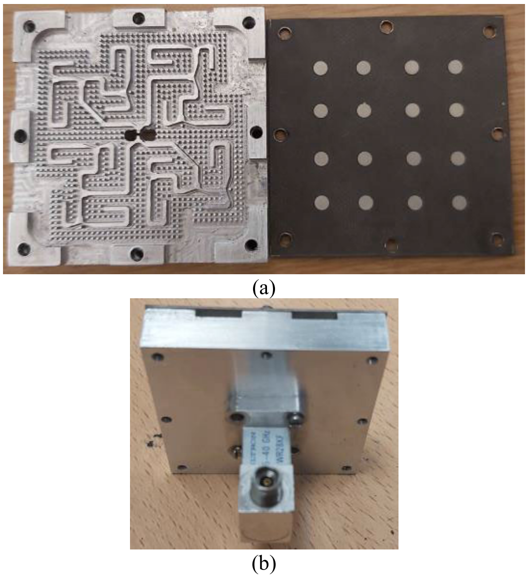

FIGURE 10. Photographs of (a) disassembled, (b) assembled fabricated antenna.

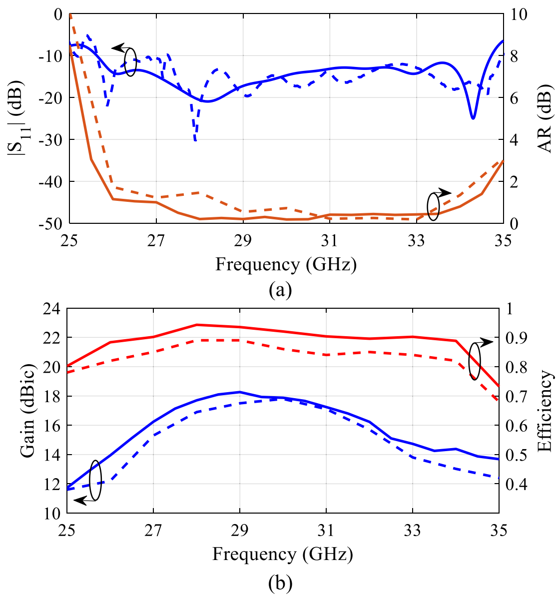

FIGURE 11. Measured and simulated results of proposed circularly polarized 4 × 4-element antenna array. (a) $|S_{11}|$ and AR. (b) Efficiency and gain. Measured values are shown with dashed-lines.

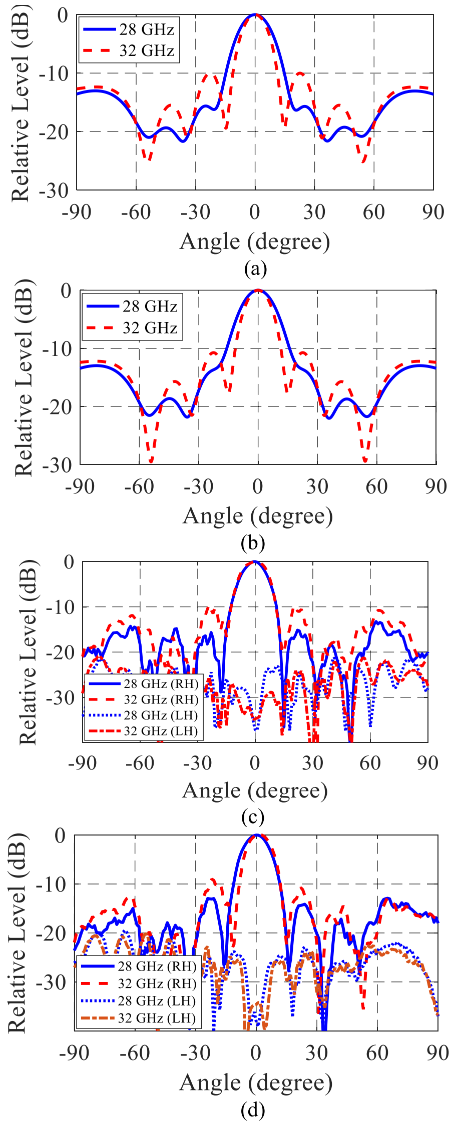

FIGURE 12. Normalized radiation patterns of CP 4 × 4-element antenna array in principal planes at 28 and 32 GHz. (a and b) Simulated. (c and d) Measured.

principal planes are about −14 dB and −10 dB at frequencies of 28 and 32 GHz, respectively. As the frequency increases, the spacing between the radiating elements increases compared to the wavelength, and so the status of the SLL become worse.The measured simulated cross polarizations level is lower than −21 dB in the two principal planes.

C. DISCUSSION

A performance comparison between the presented work and recently published articles with CP antenna arrays are presented in Table 3. The proposed design is a double layer structure consists of 1 GW-based feeding network layer and 1 substrate layer. It has acceptable IBW and ARBW bandwidth compared with similar structures. It is observed that the ohmic losses and dielectric losses of the proposed system is relatively low because of adopting the gap waveguide technology in the feeding network layer which has led to 90% radiation efficiency. Most of the reported antennas in Table 3 are either multi-layer structures or required complicated mechanical techniques for manufacturing process. In [17] and [32], antennas with bandwidths of about 40 and 49% have been reported, although structures with 4 and 7 layers have been employed in them. In addition, the reported antennas in [13], [14], [15], [16], [17], [18], [19] are based on a dielectric substrate that imposes dielectric loss to the structure and lowers the antenna efficiency. The proposed

TABLE 3. A comparison between some recently published articles with circularly polarized antenna arrays.

Ref.	No. of Elements	f_0 (GHz)	IBW (%)	ARBW (%)	Gain (dBic)	Eff. (%)	No. of layers	Dimensions (λ_0^3)
[13]	4×4	19.7	14	14	16	-	3	12×13×0.2
[14]	4×4	35.4	1.5	1.5	18.1	47	4	5×5×2
[15]	4×4	27	27.7	27.8	20.2	40-78	4	7×5×0.4
[16]	8×8	37.5	27.6	32.7	25.2	75.2	3	6×6×0.5
[17]	4×4	30	40.2	36.51	19	-	4	3×3×0.4
[18]	8×8	29	22	22.07	26.1	72.54	3	6.7×6.7×0.3
[19]	8×8	31	50	28	21	65-80	3	4.3×4.3×0.1
[30]	2×2	25.5	25.6	19	11.5	-	6	4×4×0.2
[31]	8×8	30	22	22	23.5	85	3	9×9×3
[32]	8×8	24.5	49	44.5	20.9	34-70	7	3.7×3.7×1
[33]	4×4	29.25	13.6	13.6	19.2	77-85	2	4×4×1.8
[34]	2×2	25.5	8.2	10.6	11.7	-	5	3×4×1
This Work	4×4	31	30.3	30.6	18	70-90	2	3.5×3.5×1

CP antenna array could be a proper candidate for various broadband mmWave applications.

V. CONCLUSION

In this article, a CP antenna array is presented. The radiating element is a circular patch fed with a ridge air gap waveguide. The feeding network consists of a two-level sequential feeding network in order to obtain a high polarization bandwidth. The final structure is an array with 4 × 4 elements fed by a standard WR-28 waveguide. The simulation results show an IBW of 30.6% and a polarization bandwidth of 30.3%. Based on these significant advantages, the proposed CP antenna array could be an excellent choice for mmWave applications. In the future, it is expected to generalize the proposed design to realize a dual-CP antenna array.

REFERENCES

[1] W. Hong et al., "The role of millimeter-wave technologies in 5G/6G wireless communications," *IEEE J. Microw.*, vol. 1, no. 1, pp. 101–122, Jan. 2021.

[2] H. Sun, Y.-X. Guo, and Z. Wang, "60-GHz circularly polarized U-slot patch antenna array on LTCC," *IEEE Trans. Antennas Propag.*, vol. 61, no. 1, pp. 430–435, Jan. 2013.

[3] W. Zhou, J. Liu, and Y. Long, "A broadband and high-gain planar complementary Yagi array antenna with circular polarization," *IEEE Trans. Antennas Propag.*, vol. 65, no. 3, pp. 1446–1451, Mar. 2017.

[4] Y. Li, Z. N. Chen, X. Qing, Z. Zhang, J. Xu, and Z. Feng, "Axial ratio bandwidth enhancement of 60-GHz substrate integrated waveguide-fed circularly polarized LTCC antenna array," *IEEE Trans. Antennas Propag.*, vol. 60, no. 10, pp. 4619–4626, Oct. 2012.

[5] Y. Li and K.-M. Luk, "A 60-GHz wideband circularly polarized aperture-coupled magneto-electric dipole antenna array," *IEEE Trans. Antennas Propag.*, vol. 64, no. 4, pp. 1325–1333, Apr. 2016.

[6] S. Kamal, M. F. B. Ain, U. Ullah, A. S. B. Mohammed, F. Najmi, R. Hussin, Z. A. Ahmad, M. F. B. M. Omar, M. F. A. Rahman, M. N. Mahmud, and M. Othman, "Wheel-shaped miniature assembly of circularly polarized wideband microstrip antenna for 5G mmWave terminals," *Alexandria Eng. J.*, vol. 60, no. 2, pp. 2457–2470, Apr. 2021.

[7] A. Gaya, M. H. Jamaluddin, B. Alali, and A. A. Althuwayb, "A novel wide dual band circularly polarized dielectric resonator antenna for milli meter wave 5G applications," *Alexandria Eng. J.*, vol. 61, no. 12, pp. 10791–10803, Dec. 2022.

[8] M. Akbari, S. Gupta, and A. R. Sebak, "Sequential feeding networks for subarrays of circularly polarized patch antenna," in *Proc. IEEE Int. Symp. Antennas Propag. (APSURSI)*, Jun. 2016, pp. 587–588, doi: 10.1109/APS.2016.7696002.

[9] M. S. Ibrahim, H. Attia, Q. Cheng, and A. Mahmoud, "Wideband circularly polarized aperture coupled DRA array with sequential-phase feed at X-band," *Alexandria Eng. J.*, vol. 59, no. 6, pp. 4901–4908, Dec. 2020.

[10] A. Chen, Y. Zhang, Z. Chen, and C. Yang, "Development of a Ka-band wideband circularly polarized 64-element microstrip antenna array with double application of the sequential rotation feeding technique," *IEEE Antennas Wireless Propag. Lett.*, vol. 10, pp. 1270–1273, 2011.

[11] M. H. Reddy, C. Min, N. Howland, and N. R. Potts, "A high gain 16 × 16 Ka-band circularly polarized planar array antenna," *J. Electromagn. Waves Appl.*, vol. 36, no. 9, pp. 1298–1310, Jan. 2022.

[12] Y. Lang, S.-W. Qu, and J.-X. Chen, "Wideband circularly polarized substrate integrated cavity-backed antenna array," *IEEE Antennas Wireless Propag. Lett.*, vol. 13, pp. 1513–1516, 2014.

[13] D.-F. Guan, C. Ding, Z.-P. Qian, Y.-S. Zhang, Y. J. Guo, and K. Gong, "Broadband high-gain SIW cavity-backed circular-polarized array antenna," *IEEE Trans. Antennas Propag.*, vol. 64, no. 4, pp. 1493–1497, Apr. 2016.

[14] W. Li, X. H. Tang, and Y. Yang, "A Ka-band circularly polarized substrate integrated cavity-backed antenna array," *IEEE Antennas Wireless Propag. Lett.*, vol. 18, no. 9, pp. 1882–1886, Sep. 2019.

[15] B. Feng, J. Lai, K. L. Chung, T.-Y. Chen, Y. Liu, and C.-Y.-D. Sim, "A compact wideband circularly polarized magneto-electric dipole antenna array for 5G millimeter-wave application," *IEEE Trans. Antennas Propag.*, vol. 68, no. 9, pp. 6838–6843, Sep. 2020.

[16] L. Zhang, K. Wu, S.-W. Wong, Y. He, P. Chu, W. Li, K. X. Wang, and S. Gao, "Wideband high-efficiency circularly polarized SIW-fed S-dipole array for millimeter-wave applications," *IEEE Trans. Antennas Propag.*, vol. 68, no. 3, pp. 2422–2427, Mar. 2020.

[17] Y. Cheng and Y. Dong, "Wideband circularly polarized planar antenna array for 5G millimeter-wave applications," *IEEE Trans. Antennas Propag.*, vol. 69, no. 5, pp. 2615–2627, May 2021.

[18] X.-C. Wang, Y.-J. Xia, J.-H. Yang, and W.-Z. Lu, "Wideband high-gain circularly polarized substrate integrated cavity antenna array for millimeter-wave applications," *IEEE Trans. Antennas Propag.*, vol. 71, no. 1, pp. 1041–1046, Jan. 2023.

[19] Q. Tan, K. Fan, W. Yu, Y. Yu, and G. Q. Luo, "A broadband circularly polarized planar antenna array using magneto-electric dipole element with bent strips for Ka-band applications," *IEEE Antennas Wireless Propag. Lett.*, vol. 22, no. 1, pp. 39–43, Jan. 2023.

[20] K. C. Dimitrov, Y. Lee, B.-W. Min, J. Park, J. Jeong, and H.-J. Kim, "Circularly polarized T-shaped slot waveguide array antenna for satellite communications," *IEEE Antennas Wireless Propag. Lett.*, vol. 19, no. 2, pp. 317–321, Feb. 2020.

[21] Y. Liu, X. Liang, X. Zhang, J. Li, J. Geng, R. Jin, and L. Zhang, "A K-band broadband circularly polarized slot antenna based on L-shaped waveguide cavity," *IEEE Antennas Wireless Propag. Lett.*, vol. 20, no. 9, pp. 1606–1610, Sep. 2021.

[22] H. Wang, X. Lei, T.-D. Duan, T.-P. Li, M.-Y. Zhao, J. Gao, and P. Lu, "Circularly polarized waveguide aperture array antenna with a wide axial ratio bandwidth," *IEEE Antennas Wireless Propag. Lett.*, vol. 21, no. 8, pp. 1644–1648, Aug. 2022.

[23] P.-S. Kildal, E. Alfonso, A. Valero-Nogueira, and E. Rajo-Iglesias, "Local metamaterial-based waveguides in gaps between parallel metal plates," *IEEE Antennas Wireless Propag. Lett.*, vol. 8, pp. 84–87, 2009.

[24] A. U. Zaman and P.-S. Kildal, "Wide-band slot antenna arrays with single-layer corporate-feed network in ridge gap waveguide technology," *IEEE Trans. Antennas Propag.*, vol. 62, no. 6, pp. 2992–3001, Jun. 2014.

[25] A. Vosoogh, M. S. Sorkherizi, A. U. Zaman, J. Yang, and A. A. Kishk, "An integrated Ka-band diplexer-antenna array module based on gap waveguide technology with simple mechanical assembly and no electrical contact requirements," *IEEE Trans. Microw. Theory Techn.*, vol. 66, no. 2, pp. 962–972, Feb. 2018.

[26] M. Rezaee and A. U. Zaman, "Groove gap waveguide filter based on horizontally polarized resonators for V-band applications," *IEEE Trans. Microw. Theory Techn.*, vol. 68, no. 7, pp. 2601–2609, Jul. 2020.

[27] S. Peng, Y. Pu, Z. Wu, and Y. Luo, "High-isolation power divider based on ridge gap waveguide for broadband millimeter-wave applications," *IEEE Trans. Microw. Theory Techn.*, vol. 70, no. 6, pp. 3029–3039, Jun. 2022.

[28] D. Zarifi, A. Farahbakhsh, and A. U. Zaman, "A gap waveguide-based D-band slot array antenna with interdigital feed network," *IEEE Trans. Antennas Propag.*, early access, Jun. 30, 2023, doi: 10.1109/TAP.2023.3290080.

[29] M. Ferrando-Rocher, J. I. Herranz-Herruzo, A. Valero-Nogueira, and A. Vila-Jimenez, "Single-layer circularly-polarized Ka-band antenna using gap waveguide technology," *IEEE Trans. Antennas Propag.*, vol. 66, no. 8, pp. 3837–3845, May 2018.

[30] C. Ma, Z.-H. Ma, and X. Zhang, "Millimeter-wave circularly polarized array antenna using substrate-integrated gap waveguide sequentially rotating phase feed," *IEEE Antennas Wireless Propag. Lett.*, vol. 18, no. 6, pp. 1124–1128, Jun. 2019.

[31] M. Akbari, A. Farahbakhsh, and A.-R. Sebak, "Ridge gap waveguide multilevel sequential feeding network for high-gain circularly polarized array antenna," *IEEE Trans. Antennas Propag.*, vol. 67, no. 1, pp. 251–259, Jan. 2019.

[32] T.-L. Zhang, L. Chen, S. M. Moghaddam, A. U. Zaman, and J. Yang, "Millimeter-wave ultrawideband circularly polarized planar array antenna using bold-C spiral elements with concept of tightly coupled array," *IEEE Trans. Antennas Propag.*, vol. 69, no. 4, pp. 2013–2022, Apr. 2021.

[33] M. Ferrando-Rocher, J. I. Herranz-Herruzo, A. Valero-Nogueira, and B. Bernardo-Clemente, "Single-layer sequential rotation network in gap waveguide for a wideband low-profile circularly polarized array antenna," *IEEE Access*, vol. 10, pp. 62157–62163, 2022.

[34] M. Jafari Chashmi, P. Rezaei, A. H. Haghparast, and D. Zarifi, "Dual circular polarization 2×2 slot array antenna based on printed ridge gap waveguide technology in Ka band," *AEU-Int. J. Electron. Commun.*, vol. 157, Dec. 2022, Art. no. 154433.

[35] D. Zarifi, A. Farahbakhsh, and A. U. Zaman, "Design of a dual-CP gap waveguide fed aperture array antenna," *IET Microw., Antennas Propag.*, vol. 17, no. 9, pp. 723–730, Jun. 2023.

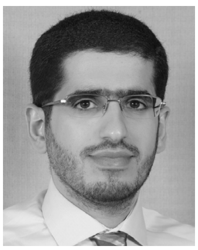

ABDULLAH J. ALAZEMI (Member, IEEE) received the B.S. degree in electrical engineering from Kuwait University, in 2010, and the M.S. and Ph.D. degrees in electrical and computer engineering from the University of California at San Diego, La Jolla, CA, USA, in 2013 and 2015, respectively. He joined the Department of Electrical Engineering, Kuwait University, in 2016. His works focus on tunable antennas and filters with RF-MEMS and MM-wave to THz quasi-optical systems, 5G reconfigurable antennas for biomedical applications, multiband power dividers, and couplers for advanced communication systems. In 2021, he received the Kuwait Award for Excellence and Creativity in Science and Technology provided by his Highness Sheikh Nawaf Al-Ahmad Al-Jaber Al-Sabah, Amir of Kuwait.

ALI FARAHBAKHSH was born in Kerman, Iran, in 1984. He received the Ph.D. degree in electrical engineering from the Iran University of Science and Technology, Tehran, Iran, in 2016. He is currently an Assistant Professor with the Department of Electrical and Computer Engineering, Graduate University of Advanced Technology, Kerman. His research interests include microwave and antenna engineering, including gap waveguide technology, millimeter-wave high-gain array antenna, microwave devices, electromagnetic waves propagation and scattering, inverse problems in electromagnetic, and anechoic chamber design.

DAVOUD ZARIFI was born in Kashan, Iran, in 1987. He received the B.S. degree from the University of Kashan, Kashan, in 2009, and the M.S. and Ph.D. degrees from the Iran University of Science and Technology (IUST), Tehran, Iran, in 2011 and 2015, respectively. He is currently an Associate Professor with the School of Electrical and Computer Engineering, University of Kashan. His research interests include metamaterials, microwave passive components, slot array antennas, and gap waveguide technology.